Mon. Not. R. astr. Soc. (1988) **232,** 821–834

The determination of wind terminal velocities and ionic abundances from infrared fine-structure lines: the WC8 component of γ Velorum

M. J. Barlow *Department of Physics and Astronomy, University College London, Gower Street, London WC1E 6BT*

P. F. Roche *Royal Observatory Edinburgh, Blackford Hill, Edinburgh EH9 3HJ*

D. K. Aitken *Physics Department, University College, ADFA, Campbell, ACT 2600, Australia*

Accepted 1987 December 17. Received 1987 December 11; in original form 1987 August 17

Summary. The spectrum of γ Velorum has been observed with a resolving power of 330 in the 12–13 μm spectral region. The 12.8 μm forbidden line of [Ne II] has a rectangular profile, as expected for an optically thin line formed at large radii. The wind terminal velocity implied by this profile is 1520 ± 200 km s^{-1}. This velocity, combined with the known radio flux, implies a mass loss rate of $8.8 \times 10^{-5}\ M_{\odot}$ yr^{-1} for γ Vel. An analysis of the He I and He II recombination lines observed in the spectrum implies that the He^{+}/He^{2+} ratio exceeds 6 in the 12 μm emitting region, confirming previous inferences that the degree of ionization decreases outwards in the wind. The flux measured in the [Ne II] line is used, along with the published [Ne III] 15.5 μm line flux, to rederive the abundance of neon in the wind of γ Vel, using improved analysis techniques. A Ne/He number ratio of $1.0 \pm 0.35 \times 10^{-3}$ is found, a factor of 9 lower than previously estimated. This neon abundance is only slightly higher than would be expected for an initial cosmic abundance ratio. The large enhancement in the abundance of neon that is theoretically predicted for WC stars, due to the creation of ^{22}Ne, is not present in the case of γ Vel.

1 Introduction

Spectroscopy in the infrared has revealed that Wolf–Rayet (WR) stars have very rich spectra with a host of bright emission lines (e.g. Williams 1982). The lines, which arise in the outflow from the star, are mostly of ions of He, C and N and analysis of the relative intensities can give the abundances of the different ionic states of the emitting elements (Hummer, Barlow & Storey 1982). In addition to the recombination lines seen in optical and near-infrared spectra, infrared collisionally excited fine-structure lines have been detected in the brightest WR star γ Vel, a binary system consisting of a WC8 Wolf–Rayet star and an O9I star [see Bidelman (1979) for a

discussion of the correct nomenclature for this system]. Emission from [S IV] and [Ne II] at 10.5 and 12.8 μm was measured by Aitken, Roche & Allen (1982, hereafter ARA) whilst the 15.5 μm [Ne III] line was detected by the low resolution spectrometer on *IRAS* (van der Hucht & Olnon 1985). Because of the effects of collisional de-excitation at high densities, the emission from the forbidden lines is weighted towards the low-density regions of the stellar wind. These regions are far from the star and correspond to the realm where the outflow has attained its terminal velocity. Measurement of the profile of the fine-structure lines will therefore yield the terminal velocity (Barlow 1982). Such infrared measurements can yield more reliable terminal velocities than is possible by using ultraviolet data, where the exact placement of blueshifted absorption edges can often be difficult. Further, because of ionization stratification in Wolf–Rayet winds, those ions with accessible ultraviolet resonance lines may not always arise in the terminal velocity regions of the flow. Finally, a resonance line from the wind of a Wolf–Rayet star that has an O star companion, e.g. γ Vel, can have its blueward line absorption edge masked by the saturated profile arising from the higher terminal velocity, but lower mass loss rate, wind from the O star.

Together with appropriate modelling, observations of the IR forbidden lines can yield the abundances of S^{3+}, Ne^{+} and Ne^{2+} and, because Ne^{+} and Ne^{2+} are expected to be the dominant ionization states of neon in most WR subtypes, the total abundance of neon relative to helium can be derived. For γ Vel, such a calculation has been published for Ne^{+} and S^{3+} by ARA and for Ne^{2+} by van der Hucht & Olnon (1985) but unfortunately, partially owing to an error in the dimensions of one of the recombination coefficients employed by ARA (which was propagated by van der Hucht & Olnon) the results obtained were incorrect.

Here, we present spectroscopy of γ Vel between 12.2 and 13.3 μm with a resolving power sufficient to measure the profiles of the emission lines. We determine the terminal velocity of the wind using the measurements of the 12.8 μm [Ne II] line and investigate the ionization balance and structure of the wind using the He^{+} and He^{2+} recombination lines. We model the radial dependence of the fine-structure level populations and, by combining these observations with the *IRAS* LRS measurement of [Ne III], calculate the abundance of neon.

2 Observations

The 12.3–13.3 μm spectrum of γ Vel was obtained with the UCL spectrometer at the $f/36$ chopping secondary focus of the Anglo-Australian Telescope in 1983 September during daylight hours. The spectrum was derived from the five highest resolution detectors of the array ($\Delta\lambda = 0.04\,\mu$m) by repeatedly stepping the grating to cover the region of interest. Wavelength calibration was with respect to known atmospheric absorption features and is accurate to better than 0.01 μm. Correction for telluric absorption was by reference to a sky emission spectrum taken along the line-of-sight to γ Vel. The instrument aperture employed was a circle 4.5 arcsec in diameter and the beam displacement was 30 arcsec. The sample interval was 0.0107 μm, and the spectral response was measured on the bright 10.52 μm [S IV] line in the planetary nebula NGC 7009 (the resolution $\Delta\lambda$ is nearly constant through the 10 μm window, and although the response is slightly different for point and extended sources, the effect is small; in any case, we show below that the emission from the [Ne II] line in γ Vel extends beyond our aperture). The instrumental FWHM measured in NGC 7009 is 0.039 μm, corresponding to a resolving power of 330 at 12.8 μm. The spectra, shown in Fig. 1, have been smoothed with a triangular function so that adjacent data points are correlated – effectively every second point is independent.

The spectral region scanned covers the positions of three emission lines found by ARA whose main contributors were identified as He I (7–6) at 12.37 μm, [Ne II] at 12.81 μm and He II (11–10) at 13.12 μm. The wavelengths and identifications are confirmed to higher accuracy and in particular the 12.8 μm line cannot be C IV 17–16 at 12.77 μm although there could be a small

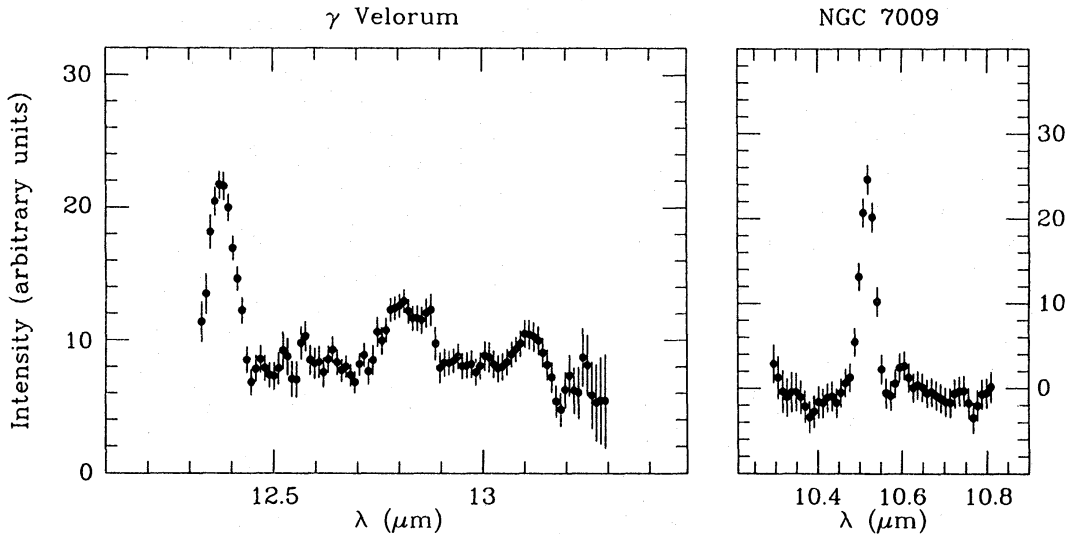

Figure 1. The 12.3–13.3 μm spectrum of γ Vel. Also shown is a scan over the 10.5 μm [S IV] line in the planetary nebula NGC7009, which gives the instrumental profile of the spectrometer.

contribution. The He I (7–6) line has contributions from He I (11–8) and He II (14–12) while the He II (11–10) line is blended with C II (11–10); these are allowed for in the discussion below. It is evident from inspection of Fig. 1 that, as predicted (Barlow 1982), the profile of the [Ne II] line is flat-topped and quite different from those of the recombination lines.

3 Emission line measurements

A standard star for flux calibration was not observed in the high-resolution mode of the UCL spectrometer during the observing run so we have used other measurements of γ Vel together with the equivalent widths from the present observations to give line fluxes.

The *IRAS Point Source Catalog* gives 12 and 25 μm fluxes of 19.42 and 8.72 Jy respectively for γ Vel. The spectral index in the mid-infrared is 1.0, so that the corrected fluxes, according to the recipe given in the *IRAS Explanatory Supplement*, are 15.5 and 7.39 Jy. γ Vel was measured in 1977 March with intermediate bandwidth filters in the 8–13 μm region, as part of the programme reported by Cohen & Barlow (1980). However, the calibrations assumed there were for room temperature, so the data have been recalibrated using the effective wavelengths for the filters when cold and a Kurucz 9400 K $\log g = 3.95$ model for Vega, which is assumed to have a magnitude of 0.00 in the 10 μm region. γ Vel was measured with respect to α CMa, for which a 10 μm magnitude of −1.35 was adopted. The revised measurements for γ Vel give 15.6 Jy at 10.4 μm and 15.1 Jy at 11.5 μm. Finally, the spectrum of ARA has a flux of 14.8 Jy at 12 μm. All of these measurements are in (surprisingly) good accord and we can confidently adopt the *IRAS* value for the 12 μm flux. Extrapolating this value to 12.8 μm with a $\nu^{1.0}$ slope gives a 12.8 μm continuum flux of 14.5 Jy or 2.7×10^{-13} Wm^{-2} μm^{-1}.

The equivalent widths, adopted continua and line intensities of the lines between 12.3 and 13.3 μm are given in Table 1. We estimate that the total uncertainties are 15 per cent for the He I and [Ne II] lines and 25 per cent for the He II + C II line. These values may be compared with those obtained by ARA with a resolution of 0.09 μm. The agreement is excellent for the two brighter lines but the intensity of the He II (11−10) + C II (11–10) line here is substantially lower; this line is at the edge of the atmospheric window and subject to greater uncertainties than the others. In view of this discrepancy, and in the absence of any other evidence, we have adopted the mean of

Table 1. Emission lines.

Line	λ (μm)	E.W. (μm)	Continuum	Line intensity	$2v_0$ km s^{-1}
[S IV]	10.52			1.9 ±0.4	
He I 7–6	12.37	0.112	29.5	3.3 ±0.46	2140±200
[Ne II]	12.81	0.062	26.6	1.7 ± 0.26	3040±400
He II 11–10 +C II 11–10	13.12	0.026	24.8	0.65±0.15	2020±400
[Ne III]	15.55			9.0 ±2.0	

Notes:

Continuum flux in 10^{-14} Wm^{-2} μm^{-1}, Line intensity in 10^{-14} Wm^{-2}. $2v_0$ is the full width of the lines after correction for the instrumental resolution. The [S IV] flux is from ARA and the [Ne III] flux from van der Hucht & Olnon (1985).

We have taken the mean of the 13.12 μm line flux quoted by ARA and that measured here, $1.0\pm0.3\times10^{-14}$ Wm^{-2}, in the analysis of the wind from γ Vel.

the 13.12 μm line flux quoted by ARA and that found here, i.e. 1.0×10^{-14} Wm^{-2}, with an estimated uncertainty of 0.3×10^{-14} Wm^{-2}, for the analysis below.

We have extracted and examined the *IRAS* LRS spectrum of γ Vel, and have adopted the intensity of the 15.5 μm [Ne III] line given by van der Hucht & Olnon (1985) of $9\pm2\times10^{-14}$ W m^{-2}.

4 The wind terminal velocity

The critical electron density for the upper level, u, of the 12.8 μm [Ne II] line is $n_c(u)=5\times10^5$ cm^{-3}, for $T_e=10^4$ K (see equation 14 of Section 7). The intensity in the transition is proportional to n_e and n_e^2, respectively, for densities much greater than and much less than the critical density and the line formation peaks in the region in the wind with $n_e=n_c(u)$ (see Table 3). This density corresponds to a radius of 9×10^{14} cm, for the mass loss rate appropriate to γ Vel (Section 5). For a typical WC8 core radius of $R_*\sim10\,R_\odot$ (Abbott *et al.* 1986), the [Ne II] line formation therefore peaks at $\sim1300\,R_*$, where we may confidently expect that the wind terminal velocity has been attained. The full width of the [Ne II] line then simply corresponds to twice v_∞

Table 2. Atomic parameters.

Ion	ν (cm^{-1})	ω_u	ω_l	A_{ul} (s^{-1})	Source	Ω_{ul}*	Source	n_u(u)* (cm^{-3})
S IV	950.2	4	2	7.75×10^{-3}	1	6.06	1	4.59×10^4
Ne II	780.4	2	4	8.55×10^{-3}	2	0.298	4	5.15×10^5
Ne III	642.9	3	5	5.97×10^{-3}	2	1.106	5	1.13×10^5
S III	535.3	5	3	2.07×10^{-3}	3	5.79	6	1.35×10^4

* $T_e=6000$ K.

Sources:

(1) Johnson, Kingston & Dufton (1986).
(2) Mendoza & Zeippen, in Mendoza (1983).
(3) Mendoza & Zeippen (1982).
(4) Bayes, Saraph & Seaton (1985).
(5) Butler & Mendoza (1984).
(6) Mendoza (1983).

and, since the line is optically thin, its profile should be flat-topped and rectangular. The observed profile of the [Ne II] line is flat-topped, with a FWZI equal to 3640 km s^{-1}, but this has been modified by the instrumental profile. In order to determine the intrinsic width of the line, we have fitted the spectrum with flat-topped profiles convolved with the spectrometer response measured on the [S IV] line in NGC 7009, and have used χ^2 tests to find the best fit. The best fit from this procedure yields an intrinsic width of 3040 ± 400 km s^{-1} corresponding to a terminal velocity of 1520 ± 200 km s^{-1}.

The full widths of the 12.37 and 13.12 μm lines, corrected for the instrumental response are 2140 ± 200 and 2020 ± 400 km s^{-1} respectively. (The contributions to the 12.37 μm line from transitions other than He I 7–6 amount to $\leqslant 10$ per cent whilst the blend between He II 11–10 and C II 11–10 at 13.12 μm is discussed in Section 6.) These velocities are significantly lower than twice the wind terminal velocity, indicating that the lines are formed in the accelerating region of the wind. The depth at which line formation occurs in the winds may be determined by either the line opacity or by the local continuum opacity. One might expect that the line opacities of the He II 11–10 and C II 11–10 and the He I 7–6 transitions would be very different, due to the very different Boltzmann factors and ionic abundances which determine the populations of the respective lower levels of these transitions. The fact that the two transitions, which are adjacent in wavelength, have identical velocity widths within the observational errors, points to the conclusion that the depth of formation of both lines is determined by the 12–13 μm free–free continuum opacity of the wind.

The terminal velocity of 1520 ± 200 km s^{-1} found for the WC8 component of γVel lies within the range for other WC8 stars determined by Torres, Conti & Massey (1986) from observations of the widths of optical recombination lines. Barlow, Smith & Willis (1981) pointed out that earlier estimates of $v_\infty = 2900$ km s^{-1} for γ Vel probably referred to the wind of the O9I component of this binary system. They instead estimated $v_\infty = 2000$ km s^{-1} for the WC8 component, from the velocity excitation potential relationship shown by the C II and C III ultraviolet absorption components, and its similarity to that of the single WC8 star HD 192103, whose ultraviolet resonance line profiles yielded $v_\infty = 2000$ km s^{-1}. Our value of $v_\infty = 1520$ km s^{-1} implies that the velocities of the C II and C III lines in fact indicate the true terminal velocity. Willis *et al.* (1979) found that the strong C II 1335 Å resonance line in the spectrum of γ Vel, which is not observed in the spectra of O9I stars, varied in phase with the WC8 component and had an edge velocity of 1600 km s^{-1}. Sahade, Kondo & McCluskey (1984) found an edge velocity of 1460 km s^{-1} for the same line. Kondo, Feibelman & West (1982) found that the redward emission edges of the strong C II, C III and C IV ultraviolet lines all fell between velocities of 1400–1660 km s^{-1}. However, their suggestion that the final terminal velocity of γ Vel could be $\sim$2600 km s^{-1} is ruled out by our observations. The 2 μm spectrum of γ Vel taken by Hillier & Hyland and published by Aitken & Roche (1983) shows that the He I $2p-2s$ line at 2.058 μm has a P Cygni profile with the minimum displaced by $\sim$1500 km s^{-1}.

It appears that all the observations can be reconciled with the terminal velocity of 1520 ± 200 km s^{-1} derived from the [Ne II] line.

5 The mass loss rate

The mass loss rate of γ Vel can be derived from its radio flux, S_ν, using the formula of Wright & Barlow (1975)

$$\dot{M} = \frac{0.095 \mu v_\infty S_\nu^{3/4} D^{3/2}}{Z \gamma_e^{1/2} g^{1/2} \nu^{1/2}} \qquad M_\odot \text{ yr}^{-1} \tag{1}$$

where the various quantities are in the units specified before equation (2) below. For γ Vel,

Barlow *et al.* (1981) assumed that the wind was pure helium (with $He^+/He^{2+}\sim1$) when estimating the mean mass per ion, μ, the rms ionic charge, Z, and the number of electrons per ion, γ_e. Recently, van der Hucht, Cassinelli & Williams (1986) have argued that carbon has a sufficiently high abundance in the winds of WC stars that mass loss rates derived from radio fluxes may be significantly larger than those derived assuming pure helium winds. In evaluating μ, Z and γ_e we have therefore adopted C/He = 0.2 by number. A value of C/He = 0.28 was derived for WC8 stars by Torres (1988), from a study of optical emission lines, while C/He = 0.12–0.28 was derived for γ Vel by Smith & Hummer (1988), from a study of infrared recombination lines. A similar C/He ratio was derived for WC stars by Nugis (1982b).

van der Hucht *et al.* (1986) have estimated that $C^{2+}/C\sim1$ in the lower regions of the winds of late-type WC stars. Combined with $He^+/He^{2+}\gg1$ (Section 6) and C/He = 0.2, this yields $\mu=5.3$, $Z=1.23$ and $\gamma_e=1.17$. A wind consisting purely of He^+ would yield exactly the same value of $\mu/Z\gamma_e^{1/2}$, while a wind with C/He = 0.5 by number would yield a value only 2 per cent higher. The main uncertainty in this quantity concerns the dominant ionization state of carbon in the radio emitting region. If C^+ rather than C^{2+} dominated, then $\mu/Z\gamma_e^{1/2}$ (and thus the derived $\dot{M}$) would be 33 per cent higher. However, the Ne^{2+}/Ne^+ ratio of 3.8 found for the radio-emitting region of the wind (Section 7) rules out C^+ as the dominant ionization stage of carbon. If C^{3+} rather than C^{2+} dominated in the radio-emitting region, then the mass loss rate would be 25 per cent lower.

In estimating a Gaunt factor of $g=4.1$ at $\nu=5\times10^9$ Hz, we have adopted the value of $T_e=6000$ K found by Hogg (1985) for the radio-emitting region of γ Vel. With $S_\nu(5\text{ GHz})=0.029$ Jy (Seaquist 1976; Hogg 1985), $D=0.46$ kpc (Conti & Smith 1972) and $V_\infty=1520$ km s^{-1} (this paper) we therefore obtain for the WC8 component of γ Vel:

$$\dot{M}=(8.8\pm2.5)\times10^{-5}\,M_\odot\text{ yr}^{-1} \tag{2}$$

with the chief source of uncertainty being the dominant ionization stage of carbon in the radio-emitting region.

Massey (1981) has estimated a mass of 20 $M_\odot$ for the WC8 component of γ Vel. A continuation of its current mass loss rate would imply that the star would lose all its mass after another 2×10^5 yr.

6 The helium recombination lines

Hummer *et al.* (1982) analysed the 2–4 μm and 8–13 μm spectra of γ Vel obtained by ARA in order to derive mean He^+/He^{2+} ratios for the emitting zones characteristic of the recombination lines in each spectral region.

The relative abundance by number, n_1/n_2, of two ions sharing the same emission region and giving rise to recombination lines with fluxes I_1 and I_2 at wavelengths λ_1 and λ_2, respectively, is given by

$$n_1/n_2=(I_1/Q_1)/(I_2/Q_2) \tag{3}$$

where $Q_i=h\nu_i\,\alpha_{\text{eff(i)}}$, and $\alpha_{\text{eff(i)}}$ (in units of cm^3 s^{-1}) is the effective recombination coefficient, at temperature T_e and electron density n_e, for the transition at wavelength λ_i.

The recombination line observed at 13.12 μm is due to He II 11–10 and C II 11–10, while the feature observed at 12.37 μm is a blend of He I 7–6 and 11–8 along with He II and C II 14–12. We can correct the 12.37 μm line flux for the He II and C II contribution using the theoretical relative Q_is for He II 11–10 and 14–12. To a very good approximation, the radiative recombination Q_is for high-n C II lines are the same as those for the analogous transitions of He II (P. J. Storey, private communication) – we shall ignore any possible contribution from dielectronic recombination to the strength of the C II lines. For the four combinations of $T_e=2\times10^4$ and 3×10^4 with

$n_e = 10^{10}$ cm^{-3} and 10^{11} cm^{-3}, the results of Hummer & Storey (1987) for He II yield Q(14–12)/Q(11–10) = 0.40 ± 0.03. We therefore estimate that 0.4×10^{-14} Wm^{-2} of the 12.37 μm line flux is due to He II and C II 14–12, leaving $(2.9 \pm 0.6) \times 10^{-14}$ Wm^{-2} due to He I 7–6 and 11–8. For the same four combinations of T_e and n_e, the mean ratio of Q(He I 7–6, 11–8)/Q(He II 11–10) is equal to 0.45 ± 0.03 (Hummer & Storey 1987, and to be published). Since I(He I 7–6, 11–8)/I(He II 11–10, C II 11–10) is equal to $2.9^{+2.1}_{-1.1}$, we obtain

$$n(\mathrm{He}^+)/[n(\mathrm{He}^{2+}) + n(\mathrm{C}^{2+})] = 6.4^{+4.6}_{-2.5}. \quad (4)$$

This ratio is slightly larger than that derived for the 8–13 μm recombination lines by Hummer *et al.* (1982), due mainly to the fact that the 13.12 μm line flux adopted here (Table 1) is lower than that estimated by ARA.

Hummer *et al.* (1982) derived a He^+/He^2 ratio of 3.8 from the recombination lines in the 1.4–4.1 μm spectrum of γ Vel observed by ARA. Smith & Hummer (1988) have derived a ratio of 2.9 from observations in the same spectral region. Torres (1988) has estimated a mean He^+/He^{2+} ratio of 2.1 for WC8 stars, from an analysis of optical recombination lines. The He^+/He^{2+} ratio of >6.4 derived here from the 8–13 μm recombination lines is therefore significantly larger than the ratios derived from the optical and 1–4 μm recombination lines. Since the wind free–free opacity ($\varkappa_\nu = \nu^{-2}$) is smaller in the optical and 1–4 μm regions than in the 8–13 μm region, one sees deeper into the wind at the shorter wavelengths. We can therefore firmly conclude that the degree of ionization of helium, in the wind of the WC8 component of γ Vel, decreases outward. Nugis (1982a) suggested a strong outward decrease in the degree of helium ionization in Wolf–Rayet winds, although his prediction of helium neutrality in the radio-emitting regions was not borne out by the detailed Wolf–Rayet models of Hillier (1987) and Schmutz & Hamann (1986), who predicted that He^+ should be the dominant ionization stage in the radio-emitting zone. In fact, our derivation of $He^+/(He^{2+} + C^{2+}) = 6.4$ and our assumption that C/He = 0.2, from the work of Torres (1988) and Smith & Hummer (1988), are consistent with the entire 13.12 μm line flux being due to C II 11–10, with helium being completely in the form of He^+. For WC8 stars, Torres estimated a mean value of 0.16 for the fraction of carbon in the form of C^{2+} in the optical emission region, while Smith & Hummer estimated a C^{2+} fraction of <0.62 for the 1–2 μm emission region of γ Vel. A C^{2+} fraction of 0.8 in the 10–13 μm region, combined with C/He = 0.2, would reproduce the ratio given by equation (4) if helium was entirely He^+.

A situation where the degree of ionization decreases outward in a wind is consistent with the main source of photoionization being the diffuse radiation field emitted by the wind itself. Consider first the case where the photoionizing flux is due to the spatially diluted photospheric radiation field, in which case the ionization rate would be inversely proportional to the square of the radius, r. If the wind has reached terminal velocity, then the electron density $n_e(r)$ will be proportional to r^{-2} also, the photoionization and recombination rates will have the same dependence on radius, and so the degree of ionization will be independent of radius (neglecting the slow build-up of optical depth in the wind). In deeper regions of the wind, which are still undergoing acceleration, $n_e(r)$ will be proportional to $[v(r)\,r^2]^{-1}$, so that the recombination rate of an ion will decrease faster with radius than will the photoionization rate and so the degree of ionization will increase with radius. Neither of these cases corresponds to the behaviour exhibited by γ Vel. Its extremely dense wind may be opaque to the central 'photospheric' ionizing radiation field, in which case the diffuse radiation field emitted by the wind itself will determine the ionization. This diffuse field arises from electron–ion collisions which give rise to line and continuum radiation. For the opaque case, the source function for the ionizing radiation field will be the Planck function corresponding to the local electron temperature. The electron temperature in Wolf–Rayet winds is known to decline with increasing radius, from values of the order of 30 000 K in the near-infrared line and continuum emitting regions (Hillier, Jones & Hyland 1982)

to values of the order of 6000 K in the radio-emitting regions (Hogg 1985). Since the ionizing continua of interest lie on the Wien tail of the Planck function, these continua will have an exponential dependence upon the electron temperature in the opaque zones of the wind, and so a decline in the degree of ionization with increasing radius is inevitable.

Another interpretation of the observed decline of the degree of ionization of helium with increasing radius comes from the work of Drew (1985, 1987), Hillier (1987) and Schmutz & Hamann (1986), where the case of stellar winds dominated by photoionization from excited states was considered in detail. When the diluted photospheric radiation field dominates, both the rate of radiative excitation to an excited state, and the photoionization rate from the excited state, will be proportional to r^{-2}, so that the overall photoionization rate will be proportional to r^{-4}. The recombination rate will be proportional to n_e as before, i.e. to $[v(r)r^2]^{-1}$. If $v(r)$ is less steep than r^2, then the degree of ionization will decline outwards. Obviously, if excited-state photoionization by the diffuse radiation field should dominate, then both of the above mechanisms will reinforce each other to speed the outward decline of ionization. At some sufficiently large radius, the wind will cease to be opaque to ionizing radiation and, if terminal velocity has been reached, the degree of ionization should remain constant thereafter. Therefore, unlike the helium recombination line formation regions, which lie in the inner part of the wind, the infrared fine-structure lines are formed at such large radii (Table 3) that the degree of ionization in the wind should be invariant over their formation region.

Table 3. IR fine-structure line emission as a function of density and radius in the wind of γ Vel. $T_e = 6000$ K.

Range of n_e (cm^{-3})	Δr(cm)	$\bar{f}_u$(SIV)	$\bar{f}_u$(SIV)Δr (cm)	$\bar{f}_u$(NeII)	$\bar{f}_u$(NeII)Δr (cm)	$\bar{f}_u$(NeIII)	$\bar{f}_u$(NeIII)Δr (cm)	$\bar{f}_u$(SIII)	$\bar{f}_u$(SIII)Δr (cm)
10^{12}–10^{8}	6.13×10^{13}	0.614	3.76×10^{13}	0.293	1.80×10^{13}	0.307	1.88×10^{13}	0.498	3.05×10^{13}
10^{8}–10^{7}	1.34×10^{14}	0.614	8.22×10^{13}	0.288	3.86×10^{13}	0.306	4.10×10^{13}	0.498	6.67×10^{13}
10^{7}–10^{6}	4.24×10^{14}	0.609	2.58×10^{14}	0.252	1.07×10^{14}	0.296	1.25×10^{14}	0.500	2.12×10^{14}
10^{6}–10^{5}	1.34×10^{15}	0.568	7.61×10^{14}	0.123	1.65×10^{14}	0.230	3.08×10^{14}	0.499	6.68×10^{14}
10^{5}–10^{4}	4.24×10^{15}	0.357	1.51×10^{15}	2.27×10^{-2}	9.61×10^{13}	8.36×10^{-2}	3.54×10^{14}	0.408	1.73×10^{15}
10^{4}–10^{3}	1.34×10^{16}	8.81×10^{-2}	1.18×10^{15}	2.52×10^{-3}	3.37×10^{13}	1.29×10^{-2}	1.73×10^{14}	0.149	2.00×10^{15}
10^{3}–10^{2}	4.24×10^{16}	1.07×10^{-2}	4.53×10^{14}	2.55×10^{-4}	1.08×10^{13}	1.40×10^{-3}	5.93×10^{13}	1.85×10^{-2}	7.83×10^{14}
10^{2}–10	1.34×10^{17}	1.10×10^{-3}	1.47×10^{14}	2.55×10^{-5}	3.41×10^{12}	1.41×10^{-4}	1.89×10^{13}	1.68×10^{-3}	2.25×10^{14}
10–1	4.24×10^{17}	1.10×10^{-4}	4.66×10^{13}	2.55×10^{-6}	1.08×10^{12}	1.41×10^{-5}	5.97×10^{12}	1.65×10^{-4}	6.99×10^{13}

7 Ionic abundances from infrared fine-structure lines and the abundance of neon in γ Vel

ARA used their data on the [Ne II] and [S IV] lines in the spectrum of γ Vel to derive the abundances of Ne^+ and S^{3+} relative to He^+. van der Hucht & Olnon (1985) used ARA's method to derive the abundance of Ne^{2+} from the [Ne III] 15.5 μm line flux observed in the LRS *IRAS* spectrum of γ Vel. We will reconsider here the excitation of fine-structure line emission in a stellar wind and we shall rederive the abundances of S^{3+}, Ne^+ and Ne^{2+} in the wind of γ Vel. These abundances will be found to be much lower (by a factor of about 10) than those derived earlier, for the following reasons:

(i) In order to derive ionic to He^+ abundance ratios, ARA and van der Hucht & Olnon normalized the strength of the infrared fine-structure lines to that of the He I 12.37 μm recombination line. As discussed in Section 4, the He I recombination lines in the 10 μm spectrum of γ Vel originate in the inner, high-density regions of its wind ($n_e > 10^{10}$ cm^{-3}) where terminal velocity has not been reached, and so the wind density distribution is steeper than r^{-2}. The infrared fine-structure lines, on the other hand, originate in the extended, lower-density, cons-

tant velocity, outer regions of the wind [critical density $n_c(u) \sim 10^4$–10^5 cm^{-3}; see Table 2] where an r^{-2} density distribution holds. This is the same region from which the observed 5 GHz radio emission originates – the use of equation (11) of Wright & Barlow (1975) implies a characteristic electron density of $\sim 2\times10^5$ cm^{-3} for the 5 GHz free–free emission region of γ Vel. In our treatment below, we will therefore normalize the observed fine-structure line fluxes to the mass loss rate given by the 5 GHz radio flux (Section 5), in order to obtain the relative ionic abundances.

(ii) ARA and van der Hucht & Olnon used theoretical fine-structure line emissivities per steradian, from Simpson (1975), but assumed that the theoretical helium recombination line coefficients of Hummer *et al.* (1982) were also per steradian, whereas recombination coefficients (e.g. those of Brocklehurst 1972) are integrated over solid angle. This led to an overestimate of all the ionic fractions by a factor of 4π.

(iii) The treatment of ARA implicitly assumed that the population of the lower fine-structure level of each transition was effectively equal to the total ionic population. This is a good assumption for planetary nebulae and H II regions, but in stellar winds 50 per cent of the flux in a fine-structure line originates from regions where n_e exceeds the critical density $n_c(u)$ (see Table 3), where a Boltzmann population distribution holds. If the statistical weight of the excited state is larger than that of the ground state (e.g. [S IV]), then most of the ionic population will be in the upper level in this region (see Table 3).

We consider a fine-structure line from ion i, with transition energy $h\nu_{ul}$. If D is the distance of the star and I_{ul} is the observed line flux, then

$$4\pi D^2 I_{ul} = \int_0^\infty n_u A_{ul} h\nu_{ul} 4\pi r^2 dr \qquad \text{erg cm}^{-2}\,\text{s}^{-1} \tag{5}$$

where A_{ul} is the line transition probability. The density of ions in the upper level, n_u, can be written as

$$n_u = f_u n_i \qquad \text{cm}^{-3} \tag{6}$$

where n_i is the density of ion species i and f_u is the population in the upper level. Thus

$$n_u = f_u \gamma_i A / r^2 \qquad \text{cm}^{-3}, \tag{7}$$

where A is the mass loss parameter:

$$A = \frac{\dot{M}}{4\pi\mu m_H v_\infty} \qquad \text{cm}^{-1} \tag{8}$$

and γ_i is the fraction of all ions represented by ion species i

$$\gamma_i = \frac{n_i}{\sum_j n_j}. \tag{9}$$

From equations (5) and (7) we obtain

$$I_{ul} = (\gamma_i / D^2)\, A_{ul} h\nu_{ul} A \int_0^\infty f_u(r)\, dr \qquad \text{erg cm}^{-2}\,\text{s}^{-1} \tag{10}$$

or

$$\gamma_i = \frac{D^2 I_{ul}}{A_{ul} h\nu_{ul} A} \frac{1}{\sum \bar{f}_u \Delta r} \tag{11}$$

where

$$\sum \bar{f}_u \Delta r = \int_0^\infty f_u(r)\, dr \qquad \text{cm}. \tag{12}$$

By using the multi-level statistical equilibrium code EQUIB (Adams 1983), along with the atomic parameters listed in Table 2, we have calculated, for the case of an r^{-2} density distribution with $T_e = 6000$ K (Hogg 1985), mean fractional upper level populations, $\bar{f}_u$ for each decade of electron density between 10^{12} and 1 cm^{-3}. These fractions are listed in Table 3 for [S IV] 10.5 μm, [Ne II] 12.8 μm, Ne III 15.5 μm and [S III] 18.7 μm. Also listed, in column 2, are the radius intervals, Δr, corresponding to each decade of electron density for γ Vel. The radius corresponding to a given electron density n_e is given by

$$r = (\gamma_e A / n_e)^{1/2} \qquad \text{cm} \tag{13}$$

where γ_e is the mean number of electrons per ion, equal to 1.17 for γ Vel, while the mass loss parameter A (equation 8) is equal to 3.28×10^{35} cm^{-1} (Section 5). For any other star, the corresponding values of Δr, for use in equation (11), can be derived if γ and A are known.

For each fine-structure line, Table 3 lists the product $\bar{f}_u \Delta r$ for each decade of electron density. By equation (10), this product traces the contribution of each density interval to the total line flux. The critical electron density for upper level u, $n_c(u)$, is defined (by Osterbrock 1974) as the density at which the sum of the downward radiative de-excitation rates are equal to the sum of the collisional excitation and de-excitation rates out of level u:

$$n_c(u) = \sum_{l<u} A_{ul} \Big/ \sum_{l \neq u} q_{ul} \qquad \text{cm}^{-3}. \tag{14}$$

The critical densities, at $T_e = 6000$ K, for the four infrared fine-structure lines of interest here, are listed in the final column of Table 2. Inspection of Table 3 shows that for each transition, the regions in the wind with $n_e > n_c(u)$ and $n_e < n_c(u)$ make equal contributions to the total line flux.

The ionic abundance fractions, γ_i can be derived for γ Vel by using equation (11) with the observed line fluxes given in Table 1, the atomic parameters from Table 2, and the values of $\Sigma \bar{f}_u \Delta r$ obtained by summing the relevant columns in Table 3. We find

$$\gamma_{S^{3+}} = 1.78 \times 10^{-5}$$

$$\gamma_{Ne^{+}} = 1.67 \times 10^{-4}$$

$$\gamma_{Ne^{2+}} = 6.57 \times 10^{-4}. \tag{15}$$

When a ground state is split into only two fine structure levels (e.g. [S IV] or [Ne II]), it is possible to derive an analytic expression for γ_i in terms of the various atomic and wind parameters. This is done in the Appendix. The ionic abundance fractions derived using equation (A13) for the case of S^{3+} and Ne^{+} are exactly equal to those in equation (15), derived by the method above. When a ground state is split into three fine-structure levels (e.g. [Ne III] or [S III]) an analytic expression analogous to (A13) is not conveniently derivable. However, for [Ne III] 15.5 μm, equation (A13) overestimates $\gamma_{Ne^{2+}}$ by only 3.7 per cent. This is because the fine-structure level not involved in the transition is the uppermost of the three, with a statistical weight of only one. However, equation (A13) would predict a $\gamma_{S^{2+}}$ from [S III] 18.7 μm which was only 81 per cent of the exact value given by the results in Table 3 – although the fine-structure level not involved in the 18.7 μm transition has a statistical weight of only one, it is the lowest level of the three and therefore has a significant population fraction at low densities.

The ionic abundances given in equation (15) assume that the flux observed in each line

represents the total emission from the wind. Therefore a correction must be made to the abundances derived for S^{3+} and Ne^{+}, in order to allow for the fact that the 4.5-arcsec beam used for the AAT observations partially resolved the wind line emission in [S IV] and [Ne II]. An angular radius of 2.25 arcsec corresponds to 1.55×10^{16} cm at 0.46 kpc, or $n_e=1.6\times10^3$ cm^{-3} from equation (13). For [S IV], 14 per cent of the total line emission originates from regions outside the cylinder projected by the spectrometer beam, while for [Ne II] the fraction is only 4 per cent. The beam of the *IRAS* LRS ensured that essentially the entire [Ne III] 15.5 μm line flux was measured by van der Hucht & Olnon (1985). The corrected ionic abundances for the wind of γ Vel are therefore

$$\gamma_{S^{3+}}=2.07\times10^{-5}$$

$$\gamma_{Ne^{+}}=1.74\times10^{-4}$$

$$\gamma_{Ne^{2+}}=6.57\times10^{-4}. \qquad (16)$$

From equations (1) and (A13), the adoption of C/He = 0.5 by number, instead of C/He = 0.2, would decrease the derived ion fractions by 9 per cent, while the adoption of C/He = 0 would increase them by the same amount. We have assumed that $C^{2+}/C=1$. As with the mass loss rate estimate in Section 5, the chief source of error in the derived ion fractions (~35 per cent) is likely to be the degree of ionization of carbon in the radio-emitting regions of the wind. (The uncertainties in the fine structure line intensities given in Table 1 are of the order of 20 per cent or less.)

The observed infrared fine-structure lines are not significantly affected by self-absorption effects. Using the wind parameters that have been derived here and the atomic constants in Table 2, one finds for the 12.8 μm [Ne II] line that a radial line-centre optical depth of unity corresponds to an inner radius of $R(\text{in})=6.5\times10^{14}$ cm, where the electron density is 10^6 cm^{-3}. In fact, 65 per cent of the total [Ne II] emission originates outside this radius (Table 3) but more importantly the bulk motions of the wind significantly reduce the effects of self-absorption. A wind temperature of 6000 K corresponds to a thermal velocity of 2.5 km s^{-1} for neon ions. For a flow speed of 1500 km s^{-1}, no line self-absorption can occur outside a cone (centred at zero radius around the flow direction of the emitting ion) having a semi-angle of $\theta=\cos^{-1}\{(1500-2.5)/1500\}=3.3°$. Averaged over all angles, the mean distance travelled by a photon before leaving this cone is $(\pi/2)\tan(\theta)\,R(\text{in})=0.091\,R(\text{in})$. The mean optical depth for self-absorption is therefore an order of magnitude less than the radial line optical depth. As a consequence, there will be no significant effect on the emitted line flux, although a narrow blue absorption edge (at $-v_\infty$) may be observable at high enough spectral resolution, due to the self-absorption of some photons emitted along the line-of-sight in a radial direction.

A 'cosmic' abundance of sulphur, corresponding to $S/H=1.6\times10^{-5}$ by number, would give $S/He=7.3\times10^{-5}$ and $\gamma_S=6.1\times10^{-5}$ if nuclear processing converted all the original hydrogen (with H/He = 10) to helium and carbon with C/He = 0.2. We have found that $\gamma_{S^{3+}}=2.1\times10^{-5}$; so if no synthesis or destruction of sulphur has occurred and the remaining sulphur is in the form of S^{2+}, equation (10) and the data in Tables 2 and 3 then predict a total [S III] 18.7 μm line flux of 8.4×10^{-15} W m^{-2}, or an equivalent width of 0.097 μm, for a continuum with a $\nu^{1.0}$ slope normalized to the *IRAS* 12 and 25 μm fluxes (Section 3). A 4.5 arcsec beam would receive only 82 per cent of the total [S III] 18.7 μm flux.

Since Ne^{2+} has an ionization potential greater than that of He^{+}, and since we have argued that $He^{+}/He^{2+}\gg1$ in the outer wind regions (Section 6), it is safe to assume that Ne^{+} and Ne^{2+} measure the total neon abundance. We therefore obtain from equation (16)

$$\gamma_{Ne}=8.3\pm3\times10^{-4}. \qquad (17)$$

For C/He = 0.2 by number, this implies $Ne/He=1.0\times10^{-3}$. An original 'cosmic' abundance of

Ne/H = 1.2×10^{-4} would give Ne/He = 5.5×10^{-4} after processing of all hydrogen to helium and beyond, with C/He = 0.2. The observed neon abundance is only a factor of 1.8 larger than this. (For C/He = 0, the neon enhancement would be a factor of 2.7, while C/He = 0.5 would imply a neon enhancement of 1.3.)

The observed enhancement of neon in γ Vel is very much smaller than that predicted by nucleosynthesis models for WC stars (e.g. Maeder 1983). These models predict that all of the initial C, N and O should be converted to ^{14}N by the CNO cycle during hydrogen burning, with the resulting nitrogen being exposed at the surface during the WN phase. During the subsequent helium burning phase, the models predict that all of the ^{14}N should be converted to ^{22}Ne via alpha-particle capture. Thus for WC stars a ^{22}Ne/^{20}Ne ratio of 10 is predicted, and a Ne/He number ratio of 6.6×10^{-3} (Maeder 1984). This is 6.6 times the number ratio that we derive. van der Hucht & Olnon (1985) had obtained Ne/He = 9×10^{-3}, in apparent agreement with theoretical predictions, but their estimate was a factor of 9 too high, for the reasons discussed at the beginning of this section.

No lines of nitrogen are seen in the WC8 spectrum of γ Vel, so the predicted conversion of all ^{14}N, by α-particle capture, has undoubtedly occurred. The lack of a significant enhancement of neon, above the level expected for the original abundance, would seem to imply that almost all of the ^{22}Ne has already been converted by further α-particle captures, at least as far as ^{25}Mg and ^{26}Mg. However, the models of Prantzos *et al.* (1986) and Maeder (1987) predict that this should not happen until the very end of the WC phase, at which point the abundance of oxygen is predicted to exceed signifiantly that of carbon. Lines of oxygen are present in the spectra of WC8 stars (e.g. Bappu 1973) but overall it is lines of carbon that dominate their spectra, apparently implying that the abundance of carbon is significantly higher than that of oxygen. The results of Maeder (1983), which used an earlier, lower value for the α-particle capture cross-section of ^{12}C, might be easier to reconcile with the observations, since they predict much lower oxygen abundances throughout the WC phase.

It may be difficult to confirm observationally that ^{22}Ne has already been transmuted to ^{25}Mg and ^{26}Mg in γ Vel. The ionization potential of Mg II is 15 eV, while that of Mg III is 80 eV. Thus the [Mg IV] 4.58 μm or [Mg V] 5.62 μm fine-structure lines (Mendoza & Zeippen 1987) are unlikely to be present. It is likely that almost all Mg will be in the form of Mg^{2+}, which has no fine-structure transitions, and very few observable transitions of any kind.

Acknowledgments

We are grateful to the SERC and PATT for support and to the staff of the AAT for their assistance. We thank J. Drew for comments on the manuscript.

References

Abbott, D. C., Bieging, J. H., Churchwell, E. & Torres, A. V., 1986. *Astrophys. J.*, **303,** 239.
Adams, S., 1983. *PhD thesis*, University of London.
Aitken, D. K. & Roche, P. F., 1984. *Galactic and Extragalactic Infrared Spectroscopy,* p. 331, eds Kessler, M. F. & Phillips, J. P., Reidel, Dordrecht, Holland.
Aitken, D. K., Roche, P. F. & Allen, D. A., 1982. *Mon. Not. R. astr. Soc.*, **200,** 69P (ARA).
Bappu, M. K. V., 1973. In: *Wolf–Rayet and High Temperature Stars, IAU Symp. No. 49*, p. 59, eds Bappu, M. K. V. & Sahade, J., Reidel, Dordrecht, Holland.
Barlow, M. J., 1982. In: *Wolf–Rayet Stars, IAU Symp. No. 99*, p. 149, eds de Loore, C. W. H. & Willis, A. J., Reidel, Dordrecht, Holland.
Barlow, M. J., Smith, L. J. & Willis, A. J., 1981. *Mon. Not. R. astr. Soc.*, **196,** 101.
Bayes, F. A., Saraph, H. E. & Seaton, M. J., 1985. *Mon. Not. R. astr. Soc.*, **215,** 85P.
Bidelman, W. P., 1979. In: *Mass Loss and Evolution of O-type Stars, IAU Symp. No. 83*, p. 137, eds Conti, P. S. & de Loore, C. W. H., Reidel, Dordrecht, Holland.

Brocklehurst, M., 1972. *Mon. Not. R. astr. Soc.*, **157,** 211.
Butler, K. & Mendoza, C., 1984. *Mon. Not. R. astr. Soc.*, **208,** 17P.
Cohen, M. & Barlow, M. J., 1980. *Astrophys. J.*, **238,** 585.
Conti, P. S. & Smith, L. F., 1972. *Astrophys. J.*, **172,** 623.
Drew, J. E., 1985. *Mon. Not. R. astr. Soc.*, **217,** 867.
Drew, J. E., 1987. *Astrophys. J.*, submitted.
Hillier, D. J., 1987. *Astrophys. J. Suppl.*, **63,** 947.
Hillier, D. J., Jones, T. J. & Hyland, A. R., 1982. *Astrophys. J.*, **271,** 221.
Hogg, D. E., 1985. In: *Radio Stars*, p. 117, eds Hjellming, R. & Gibson, D., Reidel, Dordrecht, Holland.
Hummer, D. G. & Storey, P. J., 1987. *Mon. Not. R. astr. Soc.*, **224,** 801.
Hummer, D. G., Barlow, M. J. & Storey, P. J., 1982. In: *Wolf–Rayet Stars, IAU Symp. No. 99*, p. 149, eds de Loore, C. W. H. & Willis, A. J., Reidel, Dordrecht, Holland.
Johnson, C. T., Kingston, A. E. & Dufton, P. L., 1986. *Mon. Not. R. astr. Soc.*, **220,** 155.
Kondo, Y., Feibelman, W. A. & West, D. K., 1982. *Astrophys. J.*, **252,** 208.
Maeder, A., 1983. *Astr. Astrophys.*, **120,** 113.
Maeder, A., 1984. *Adv. Space Res.*, **4,** 55.
Maeder, A., 1987. *Astr. Astrophys.*, **173,** 247.
Massey, P. M., 1981. *Astrophys. J.*, **246,** 153.
Mendoza, C., 1983. In: *Planetary Nebulae, IAU Symp. No. 103*, p. 143, ed. Flower, D. R., Reidel, Dordrecht, Holland.
Mendoza, C. & Zeippen, C. J., 1982. *Mon. Not. R. astr. Soc.*, **199,** 1025.
Mendoza, C. & Zeippen, C. J., 1987. *Mon. Not. R. astr. Soc.*, **224,** 7P.
Nugis, T., 1982a. In: *Wolf–Rayet Stars, IAU Symp. No. 99*, p. 127, eds de Loore, C. W. H. & Willis, A. J., Reidel, Dordrecht, Holland.
Nugis, T., 1982b. In: *Wolf–Rayet Stars, IAU Symp. No. 99*, p. 131, eds de Loore, C. W. H. & Willis, A. J., Reidel, Dordrecht, Holland.
Osterbrock, D. E., 1974. *Astrophysics of Gaseous Nebulae*, p. 53, W. H. Freeman, San Francisco.
Prantzos, N., Doom, C., Arnould, M. & de Loore, C., 1986. *Astrophys. J.*, **304,** 695.
Sahade, J., Kondo, Y. & McCluskey, G. E., 1984. *Astrophys. J.*, **276,** 281.
Schmutz, W. & Hamann, W. R., 1986. *Astr. Astrophys.*, **166,** L11.
Seaquist, E. R., 1976. *Astrophys. J.*, **203,** L35.
Seaton, M. J., 1958. *Rev. Mod. Phys.*, **30,** 979.
Simpson, J. P., 1975. *Astr. Astrophys.*, **39,** 43.
Smith, L. F. & Hummer, D. G., 1988. *Mon. Not. R. astr. Soc.*, **230,** 511.
Torres, A., V., 1988. *Astrophys. J.*, **325,** 759.
Torres, A. V., Conti, P. S. & Massey, P., 1986. *Astrophys. J.*, **300,** 379.
van der Hucht, K. A. & Olnon, 1985. *Astr. Astrophys.*, **149,** L17.
van der Hucht, K. A., Cassinelli, J. P. & Williams, P. M., 1986. *Astr. Astrophys.*, **168,** 111.
Williams, P. M., 1982. In: *Wolf–Rayet Stars, IAU Symp. No. 99*, p. 73, eds de Loore, C. W. H. & Willis, A. J., Reidel, Dordrecht, Holland.
Willis, A. J., Wilson, R., Macchetto, F., Beeckmans, F., van der Hucht, K. A. & Stickland, D. J., 1979. In: *The First Year of IUE*, p. 394, ed. Willis, A. J., University College London.
Wright, A. E. & Barlow, M. J., 1975. *Mon. Not. R. astr. Soc.*, **170,** 41.

Appendix: The flux in a stellar wind fine-structure line: the case of a two-level atom

Consider the case of an ion with only two ground state fine-structure levels, with energy separation $h\nu_{ul}$; the lower level l has statistical weight ω_l and the upper level u has statistical weight ω_u. The total density of ion species i is given by the sum of the populations of the two levels:

$$n_i = n_u + n_l. \tag{A1}$$

The upwards and downwards collisional rates, q_{lu} and q_{ul}, are given by (see Seaton 1958):

$$q_{ul} = \frac{8.63\times10^{-6}\,\Omega_{ul}(T_e)}{\omega_u T_e^{1/2}} \qquad \mathrm{cm^3\,s^{-1}}, \tag{A2}$$

$$q_{lu} = \frac{8.63\times10^{-6}\,\Omega_{ul}(T_e)}{\omega_l T_e^{1/2}} \exp(-h\nu_{ul}/kT_e) \qquad \mathrm{cm^3\,s^{-1}}, \tag{A3}$$

where $\Omega_{ul}(T_e)$ is the Maxwell averaged effective collision strength at electron temperature T_e. The electron density n_e, and the density of an ion species i, are given by

$$n_e = \gamma_e A/r^2 \qquad \text{cm}^{-3}, \tag{A4}$$

$$n_i = \gamma_i A/r^2 \qquad \text{cm}^{-3}, \tag{A5}$$

where the mass loss parameter A and the ion fraction γ_i are defined by equations (8) and (9) respectively, while γ_e is the mean number of electrons per ion. The equation of statistical equilibrium between the two levels can be written as

$$n_l q_{lu} n_e = n_u A_{ul} + n_u q_{ul} n_e \tag{A6}$$

or

$$n_u = n_l \left(\frac{q_{lu} n_e}{A_{ul} + q_{ul} n_e} \right) \tag{A7}$$

where A_{ul} is the spontaneous transition probability from the upper level. The critical density $n_c(u)$ corresponds to the case where the radiative and collisional de-excitation rates on the right-hand side of (A6) are equal, i.e.

$$n_c(u) = A_{ul}/q_{ul} \qquad \text{cm}^{-3}. \tag{A8}$$

Combining equation (A7) with equations (A1)–(A3) and (A8), we obtain

$$n_i = n_u + n_u \left[\frac{n_c(u) + n_e}{n_e(\omega_u/\omega_l) \exp(-h\nu_{ul}/kT_e)} \right]. \tag{A9}$$

The line flux I_{ul} received at the Earth is given by

$$I_{ul} = (1/D^2) \int_0^\infty n_u A_{ul} h\nu_{ul} r^2 \, dr. \tag{A10}$$

Substituting for n_u from equation (A9) and for n_e and n_i from equations (A4) and (A5), we obtain

$$I_{ul} = \int_0^\infty \frac{\gamma_i A}{r^2 D^2} \frac{(\omega_u/\omega_l) \exp(-h\nu_{ul}/kT_e) \, A_{ul} h\nu_{ul} r^2 \, dr}{[1 + (\omega_u/\omega_l) \exp(-h\nu_{ul}/kT_e) + n_c(u) r^2/\gamma_e A]} \tag{A11}$$

which gives

$$I_{ul} = \frac{\pi}{2} \gamma_i \gamma_e^{1/2} \frac{A^{3/2}}{D^2} h\nu_{ul} \frac{A_{ul}^{1/2} \omega_u^{1/2}}{T_e^{1/4} \omega_l} \cdot \frac{[8.63 \times 10^{-6} \Omega_{ul}(T_e)]^{1/2} \exp(-h\nu_{ul}/kT_e)}{[1 + (\omega_u/\omega_l) \exp(-h\nu_{ul}/kT_e)]^{1/2}}. \tag{A12}$$

This also gives an expression for the ion number fraction γ_i:

$$\gamma_i = \frac{2D^2 I_{ul}}{\pi \gamma_e^{1/2} A^{3/2} h\nu_{ul}} \cdot \frac{T_e^{1/4} \exp(h\nu_{ul}/kT_e)}{[8.63 \times 10^{-6} \Omega_{ul}(T_e) A_{ul}]^{1/2}} \cdot \frac{\omega_l}{\omega_u^{1/2}} \left[1 + \frac{\omega_u}{\omega_l} \exp\left(\frac{-h\nu_{ul}}{kT_e} \right) \right]^{1/2}. \tag{A13}$$